2010 IEEE International Conference on Robotics and Automation
Anchorage Convention District
May 3-8, 2010, Anchorage, Alaska, USA

Active Force Control for Robotic Micro-Assembly: Application to Guiding Tasks

Kanty Rabenorosoa, Cédric Clévy, *Member, IEEE*, and Philippe Lutz, *Member, IEEE*

***Abstract*— This paper presents an analytical model and experimental results from a study of guiding tasks in micro-assembly. This work is focused on the use of two fingers for gripping microparts. The stability of the grasp when the contact appears is investigated and strategies during the guiding task are discussed. The contact side detection and the contact force estimation are studied. The incremental control in static mode is then investigated for controlling the guiding task. Experimental setups are proposed and some experimental results are presented.**

I. Introduction

The integration of MEMS (Micro Electro Mechanical SystemS) and MOEMS (Micro Opto Electro Mechanical SystemS) technology in commercial products is growing especially in the field of telecommunication and sensor technology [1]. Heterogeneous microparts produced from various fabrication processes are frequently used for producing complex 3D microstructures through microparts micro-assembly tasks for example [2], [3], [4]. The use of a robotic workstation at the microscale which comprises a micromanipulator, high precision positioning stages, a set of visual systems and microforce sensors is commonly practiced. Micro-assembly of microparts is usually carried out by precise positioning but this approach is not sufficient for all of the micro-assembly tasks [5]. Indeed, the control of the position in a short range does not permit the control of interaction forces between the microgripper and the micropart. To avoid the destruction of microparts, a control of the grasping force is often employed. In addition, the integration of the micropositioning sensors on the microgripper is hampered by the volume of sensors [6]. Forces dominating micromanipulation of micropart smaller than 0.1 mm^3 are in the range of tens of micro-Newton up to several hundreds of micro-Newtons (when planar contacts are considered) [7], [8]. In the literature, many studies have been done on using the force control for improving the assembly tasks. Due to the fragility of the objects and the microgrippers, significant researches have been reported on controlling impact forces [9], [10], [11] and on ensuring stable grasp of microparts during micro-assembly [12], [13], [14], [15]. For succeeding in insertion tasks, force control constitutes chosen solutions like [16], [17] and [18]. For complete micro-assembly tasks based on force control, controlling both the gripping force and the contact force with the environment is not yet fully available.

Authors are with FEMTO-ST Inst., UMR CNRS 6174 - UFC / ENSMM / UTBM, Automatic Control and Micro-Mechatronic Systems depart.(AS2M department), Besancon, France rkanty, cclevy, plutz @femto-st.fr

In previous work [19] we designed RFS-MOB (Reconfigurable Free Space Micro-Optical Benches) that are based on generic components. This principle can be easly used to design various MOEMS (μspectrometer, coupling system, μ-confocal microscope...) and test benches (characterization of microcomponents). To assemble RFS-MOB its required to use grasp force control with two sensorized fingers for guiding tasks. It consists in the displacement of a micropart held by a microgripper in a rail with a given play. The paper is organized as follows. Section 2 describes the model of sensorized grasping during micro-assembly. In order to control the contact force, section 3 deals with the detection of contact and the evaluation of the contact force during the guiding task. The hybrid force/position control of the micropart is presented in section 4. Experimental results on the evaluation of the contact force and the applied controller are proposed in Section 5. Finally section 6 concludes the paper and presents future works.

II. Model of sensorized grasping

In this section, we propose a model of sensorized grasping during the guiding task. This model enables to establish grasping force conditions for succeding tasks and to deduce the guiding strategy.

A. Guiding system and steps

For performing guiding tasks, the micropart is grasped by two sensorized fingers (Fig. 1). This type of microgripper is largely used for micro-assembly. Each finger has to move in Y for ensuring the open/close of the microgripper. Here it is mounted on a high resolution XYZ stages. Each finger of the microgripper is the tip of a capacitive force sensor (S270 from FemtoTools). This compact probe sensor has a measuring range from 0 up to 2000 μN with 0.4 μN in resolution. A relative motion along X between the micropart and the rail is generated to achieve the desired position. The correction of the trajectory along Y ensures the control of the contact force. The manipulated object measures 1500 μm x 1000 μm x 100 μm.

A guiding task can be split in 7 steps (Fig. 2). Step 1 is the initial situation to start the task. The fingers come in contact with the micropart for applying a gripping force along Y (preload force, Step 2). The pick operation is operated by moving down the substrate (Step 3). The insertion of the grasped micropart in the rail is carried out by moving up the rail attached to the substrate (Step 4). Step 5 is characterized by the relative displacement of the micropart and the rail along X (guiding direction). When the contact appears (Step

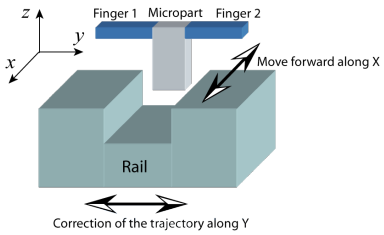

Fig. 1. Principle of a guiding task in a rail

6), the trajectory correction is applied (correction of the position in the guide along Y using force feedback). At the desired position, fingers are moved back (opening motion) for releasing the micropart (Step 7).

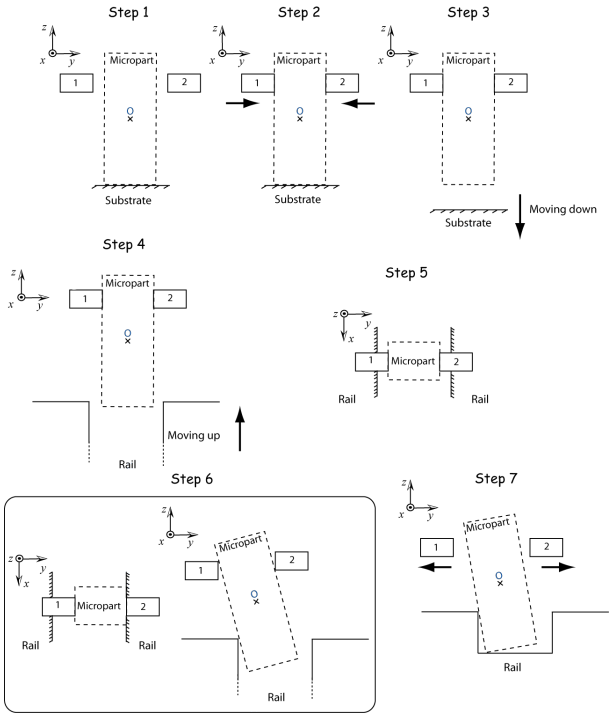

Fig. 2. The steps which are achieved during the guiding task

B. Model of the pick

We consider a micropart with rigid body which is hold by a sensorized microgripper (Fig. 1). The model of the grasp is established for a static case in the YZ plane. The microgripper which holds a micropart is represented by two fingers (here the force sensors) which behaviors can be modeled by a linear spring, a linear bond and a flexible cantilever along Z (Fig. 3). This flexibility is due to the dimensions of the cantilever that are 3000 μm x 300 μm x 50 μm. The tips of the microgripper are planar surfaces (50 μm x 50 μm) generating a planar contact with the micropart. We assume that geometry defaults (alignement of the probe: offset and tilt in XY and YZ) between the two fingers of the microgripper are negligible.

The micropart is initially placed on the subtrate and maintained vertically in Step 1. Each finger is moved towards

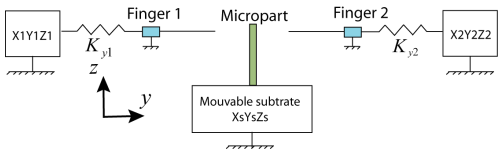

Fig. 3. Model of the microgripper with its two fingers

the micropart for applying the gripping force (Step 2). For succeeding in the grasping, the static equations are derived in taking into account that the weight is negligible. When the movable substrate is going down along Z (Step 3), the grasping forces have to overcome adhesion forces between the micropart and the substrate. Fig. 4 illustrates a simplified body diagram that is used to obtain force equations and pick condition. Lets note that F_{y1} and F_{y2} are applied forces

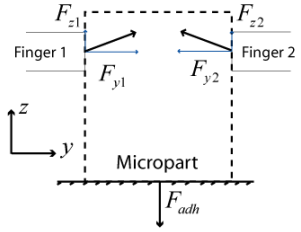

Fig. 4. Gripping force for ensuring the grasp

by Finger 1 and Finger 2 to the object along Y, F_{z1} and F_{z2} are forces induced to friction, F_{adh} the adhesion force between the substrate and the micropart , and μ the friction coefficient. When the equilibrium of the micropart is studied, the Coulomb model gives:

$$F_{y1} = F_{y2}, F_{z1} = \mu F_{y1}, F_{z2} = \mu F_{y2} \quad (1)$$

The condition of the pick (removing of the contact between the micropart and substrate) is established:

$$F_{z1} + F_{z2} > F_{adh} \quad (2)$$

Using Eq. (1), and Eq. (2), we can write:

$$\mu F_{y1} + \mu F_{y2} \quad > \quad F_{adh} \quad (3)$$

When the micropart and the substrate are separated (Step 3), the equilibrium of the micropart is obtained if the gripping forces are equal and opposite along the same line.

C. Grasp stability

During Step 5 and Step 6 (Fig 2, the stability of the grasp has to be ensured. Indeed, when a contact appears, the grasp is perturbated due to the contact force. As a result, the micropart can slip through the fingers and can be lost. We consider separately the contact force F components: F_x, F_y, and F_z and we determine the gripping force to apply according to the contact force for ensuring the stability of the grasp.

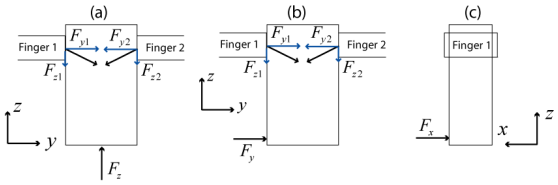

Fig. 5. Perturbated grasp with (a) F_z, (b) F_x, (c) F_z

1) Stability according to F_z perturbation (Fig. 7(a)): According to the Coulomb friction, the slidding does not happen if the tangential forces applied by the fingers are important. The condition is $2\mu F_y \geq Fz$ with $F_{y1} = F_{y2} = F_y$.

2) Stability according to F_y perturbation (Fig. 7(b)): The force F_y induces the displacement of the object between the two fingers but the object is maintained. The maximum admissible force F_y corresponds to the breaking of the fingers due to the generated torque.

3) Stability according to F_x perturbation (Fig. 7(c)): F_x induces a torque that can cause the rotation of the micropart. To prevent from this rotation, the admissible force F_y can be calculated. The surface in contact (between fingers and object) is square with 50 μm of side. We consider the circle (R: radius) with the equivalent surface (S), F_{yi} the applied force by the finger to the micropart, P the uniform pressure induced by F_{yi}, dS the elementary surface, $\overrightarrow{dN}$ and $\overrightarrow{dT}$ the elementary normal and tangential force vector respectively (Fig. 6). Note that ℓ is the distance of the applied force F_x to the center of the rotation and $\overrightarrow{n}$ is the normal unit vector.

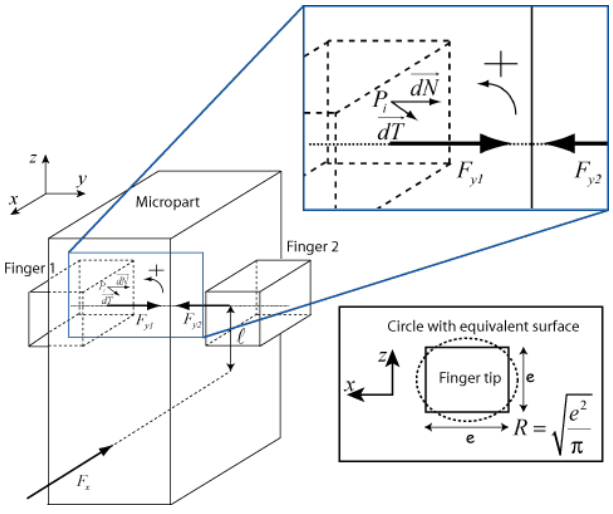

Fig. 6. Detailled scheme used for the calcul of the limit force F_x before rotation

$$F_{yi} = P.S \quad (4)$$

$$\overrightarrow{dN} = P.dS.\ \overrightarrow{n} \quad (5)$$

The condition of non sliding in a elementary considered point P_i is

$$\left\|\overrightarrow{dT}\right\| \leq \mu.P.dS. \left\|\overrightarrow{n}\right\| \quad (6)$$

According to the elementary torque dC, the integration for the complete surface gives the torque for one finger:

$$dC = \rho \left\|\overrightarrow{dT}\right\| => C = \frac{2}{3} F_{yi} \mu R \quad (7)$$

The condition of the stability is thus:

$$F_x \leq \frac{4F_{yi}\mu R}{3\ell} \quad (8)$$

D. Guiding strategies

During the Step 5, the object is moved unconstrained in the rail with a fixed velocity. When a contact on the side of the rail happens (Step 6), there are two strategies for continuing the task:

- Leave the contact and moved forward simultaneously. In that case, the gripping force must comply the condition in the Eq. (8).
- Stop the motion along X and correct the trajectory along Y by leaving the contact. After that the manipulator can be moved forward along X again.

According to the stability of the grasp in Eq. (8), the limit force F_x for ensuring the stable grasp according to F_{y1}= F_{y2}= 1100 μN, μ = 0.3, ℓ=500 μm and R=28.2 μm is estimated to $F_x \leq$ 24.8 μN. Consequently, the last strategy is chosen in the following.

III. Detecting contact during guiding task

The objective of this section is the contact side detection and the contact force estimation. For this purpose, two sensorized fingers are used and some assumptions are proposed.

A. Gripping force vs. contact force

During the guiding task, the contact between the micropart and the rail appears and creates a force $F = F_x, F_y, F_z$ at the distance ℓ. We assume that the components of F along X and Z are negligible. The evolution of the gripping forces (F_{y1} and F_{y2}) is studied according to the contact force F_y (see Fig. 7). The model of the microgripper shown in Fig. 3 is used. We define $(\Delta_{yi}, \Delta_{zi})$ the displacement of the finger $i = 1, 2$ (points A and B) in Y and Z, Δ_{yfi} the decrease along Y of the sensor cantilever due to its flexion, $F_{za} = F_{z1} = F_{z2}$ the induced force to friction along Z, c_1 the width of the micropart, e the thickness of the finger, L length of the sensor cantilever, E young module of the silicon, I the quadratic moment of the cantilever.

A system of 5 equations enables to determine Δ_{y2}, Δ_{y1}, $\Delta_z = \Delta_{zi}$, F_{za}, and $\Delta_{yf} = \Delta_{yfi}$.

The equilibrium of forces along Y gives:

$$F_y = K_y(\Delta_{y2} - \Delta_{y1}) \quad (9)$$

The expression of the cantilever flexion along Z gives:

$$\Delta_z = 0.85Lsin(\frac{0.85F_{za}L^2}{2.25EI}) \quad (10)$$

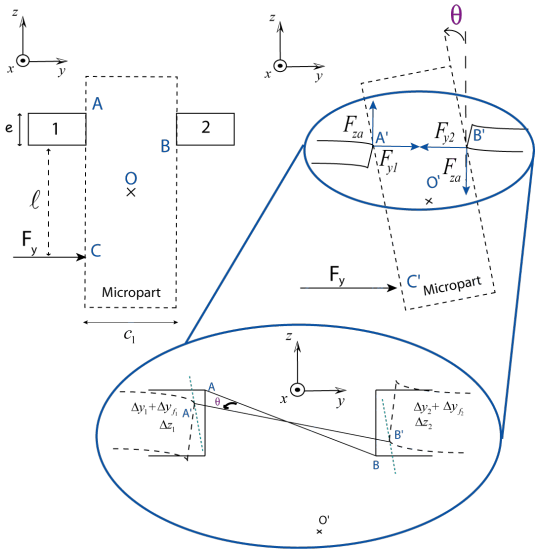

Fig. 7. Grasp before and after the apparition of F_y

The decrease along Y of the sensor cantilever due to its flexion gives:

$$\Delta_{yf} = 0.85L(1 - cos(\frac{0.85F_{za}L^2}{2.25EI})) \tag{11}$$

The torque equilibrium at the point A' gives:

$$\left\|\vec{F_y}\right\| \wedge \left\|\vec{C'A'}\right\| = \left\|\vec{F_{za}}\right\| \wedge \left\|\vec{B'A'}\right\| + \left\|\vec{F_{y2}}\right\| \wedge \left\|\vec{B'A'}\right\| \tag{12}$$

$$\begin{aligned} F_y(d + e - \Delta_z) = F_{za}(c_1 + \Delta_{y1} + \Delta_{y2} + 2\Delta_{yf}) \\ +(F_{y20} + K_y\Delta_{y2})(e - 2\Delta_z) \end{aligned} \tag{13}$$

The condition of non slipping of the object, $\left\|\vec{AB}\right\| = \left\|\vec{A'B'}\right\|$ gives:

$$4e\Delta_z - 4\Delta_z^2 = (\Delta_{y1}+\Delta_{y2}+2\Delta_{yf})^2+2c_1(\Delta_{y1}+\Delta_{y2}+2\Delta_{yf}) \tag{14}$$

The numerical resolution of this system gives the evolution of the gripping forces according to the applied contact force in Fig. 8. These curves show that the gripping force on the two fingers are not equal when the contact force is applied. The finger on the opposite side of the contact applied the biggest force to the micropart. Consequently, the side of the contact can be distinguished. This model enables to predict the behavior of the system, it will be used for the control of the contact force.

B. Evaluation of the contact force by two sensorized fingers

The proposed model shows that the contact force F_y can be evaluated from the force equilibrium along the Y axis (Eq. (15)) by using the information from two sensorized fingers.

$$F_y = F_{y2} - F_{y1} \tag{15}$$

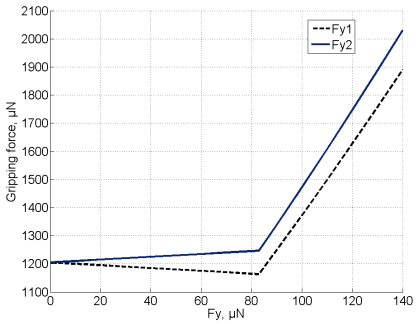

Fig. 8. Simulation results of gripping forces evolution according to F_y with $F_{y10} = F_{y20}$= 1200 μN, ℓ= 700 μm, c_1=100 μm, e=50 μm, K_y=1000 N/m, E= 170 GPa, L=3000 mm, w=300 μm

Force sensors used are coupled (the measurement depend on the force applied in the Y direction but also along Z direction). The expression of the force on the sensorized fingers are $F_{c1} = F_{y1} + \alpha F_{z1}$ (Finger 1) and $F_{c2} = F_{y2} + \alpha F_{z2}$ (Finger 2) where α is the coupling coefficient. Consequently,

$$F_y = F_{c2} - F_{c1} - \alpha F_z \tag{16}$$

The coupling coefficient is small ($\alpha = 0.01$ given by FemtoTools). F_z is also small during the contact, αF_z becomes negligible thus the contact force F_y can be evaluated:

$$F_y = F_{c2} - F_{c1} \tag{17}$$

IV. Hybrid force/position control of the object

For controlling the guiding task in automated mode, a control of the system is established. The objective of this control is to remove the contact using the measure of the gripping forces. According to results in subsection II-D, the position control along the rail and the contact force have to be separated thus the use of hybrid control like [20] and combined with [9] is chosen. The proposed block diagram (Fig. 9) enables to control the position in X (move forward) and to remove the contact in Y. Indeed, $X_d = [X, Y, Z]$ is the input position of the 3 DOF robot, F_d is the input contact force ($F_d = 0$ in our case). The matrix of selection **S** enables the position control along the X and Z axis:

$$\begin{bmatrix} 1 & 0 & 0 \\ 0 & 0 & 0 \\ 0 & 0 & 1 \end{bmatrix}$$

In the following we focus on the force control loop and propose an incremental static control (Fig. 10) for ensuring the Force Control Law (FCL). The proposed controller enables easy and fast set up of parameters and reduces risks of breaking components or parts of the manipulator. It is composed of a dead zone for rejecting the sensor noise measurement ($\approx 15\ \mu N$), the sign operator indicates the sense of the increment, the memory operation enables the relative positionning. Indeed the robot is a direct-drive position control actuated by piezo stack. The controller gives the absolute position control along Y to the manipulator. This

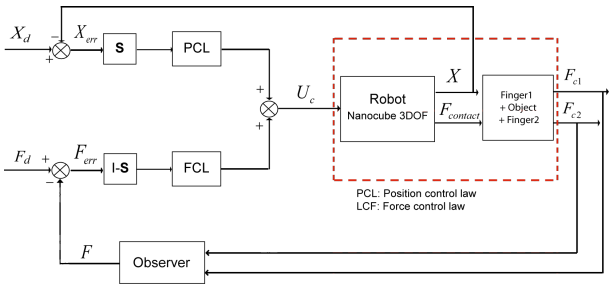

Fig. 9. Block diagram of the hybrid force/position control during the guiding task

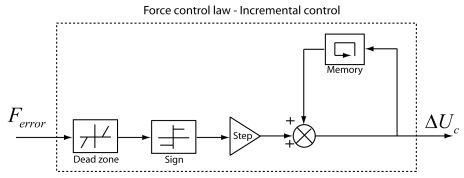

Fig. 10. Details of the incremental controller (FCL)

controller is implemented and the experimental validation is proposed.

V. Experimental results

A. Measurement of the contact force F_y

The objective of this section is the comparison of the estimated contact force F_y according to the assumption in section III and the applied contact force. Consequently a third force sensor is used instead of the rail enabling the measurement of the contact force. Due to the obstruction of the two fingers of the microgripper, it is not possible to use the same sensor (S270 FemtoTools). The proposed setup needs the modification of the sensor design by rotate in 90° the active part of the sensor. This change necessitates welding and calibration of the new sensor (called "perpendicular sensor"). The calibration of this perpendicular sensor is done with the conventional $S270$ FemtoTools and permits to establish the sensitivity of the perpendicular sensor (S_{ps}= 1743 μN, the stiffness is not affected).

The validation of the measurement of the contact force F_y is done by using the setup measurement shown in Fig. 11. This is composed of two $S270$ mounted on the $X_iY_iZ_i$ stages which constitute the microgripper, a movable substrate (is also mounted on the fine stage $X_sY_sZ_s$ Nanocube) and the perpendicular sensor mounted on the $X_cY_cZ_c$ coarse stage. Fig. 12 shows the evolution of the gripping forces (F_{c1}, F_{c2}) and the comparison of the measured applied contact force $F_{y\ measured}$ and the estimated contact force $F_{y\ estimated}$(using Eq. (17)). The estimated force is equal to the measured force in static part. This result validates the assumptions made in section III. The measured force is affected by a slow dynamic part due to the fact that we added wire and welding between the active part of the sensor and the readout circuit.

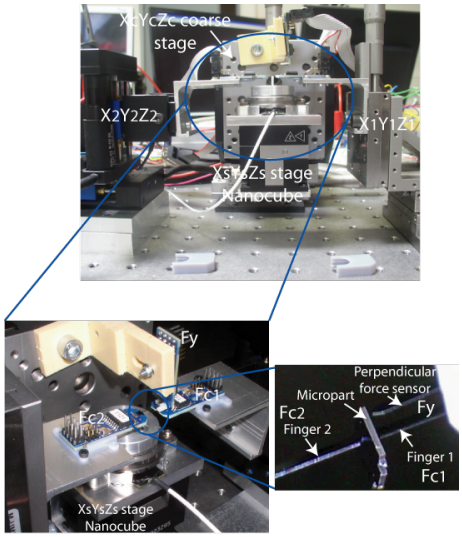

Fig. 11. Setup measurement of F_y by using perpendicular sensor

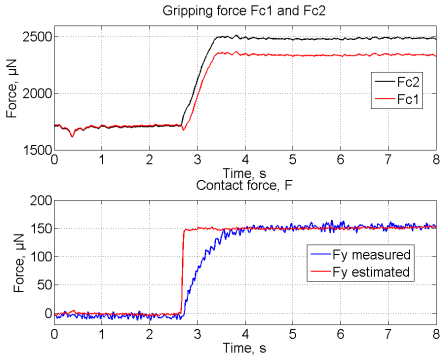

Fig. 12. Estimation of the contact force $F_{yestimated}$ by using F_{c1} and F_{c2} compared to the applied contact force $F_{ymeasured}$

B. Validation of the incremental control

For validating the incremental control, the movable substrate perturbates the grasped micropart when the controller is turned off (Fig. 13). The contact force F_y is not yet measured. During this validation, the measurement is focused on:

- the generation of the perturbation by actuating Y_s axis,
- the observation of the gripping forces evolution,
- the estimation of the contact force F_y,
- the activation of the controller,
- the observation of the correction effect.

The proposed incremental control is implemented on a 1103 Dspace board with a sampling frequency $F_{sampling} = 25Hz$. The results are shown on Fig. 14. The controller is activated and the estimated contact force decreases until the dead zone [-20:20] μN is reached. A residual contact force is maintained due to the dead zone but the induced friction force (along X) is smaller than the limit force calculated in subsection II-D ($F_x \leq 24.8$ μN) then the grasp stability is ensured.

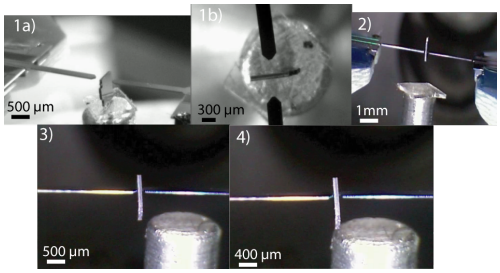

Fig. 13. Sequence during the validation of the incremental control: 1a) and 1b) correspond to the Step 1, 2) after that the preload force is applied (Step 2), the movable substrat is moving down (Step 3), 3) the micropart is aligned to the movable substrate, 4) the micropart is in contact with the substrate, F_y is estimated, and the correction can work

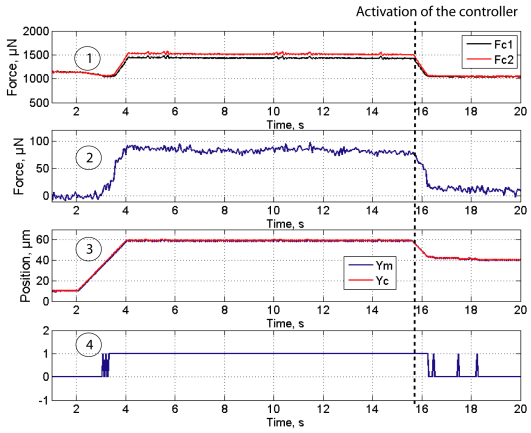

Fig. 14. Incremental control validation with step= 1 μm: (1) the variation of the measured gripping force F_{c1} and F_{c2}, (2) estimated contact force $F_y = F_{c2} - F_{c1}$, (3), Y_c desired position of along Y and Y_m the measured position along Y, (4) output of the sign operation

VI. Conclusion

In this paper, the guiding task based on two sensorized fingers ensuring the grasp during micro-assembly is discussed. The complete sequence of the guiding task is studied and the static model of two fingers grasp is proposed. The stability conditions during the task are investigated and conduct to a limit value of the contact force F_x according to the gripping force. According to this result, the guiding strategy is to stop the motion along X when the contact force F_y is bigger than the fixed limit (dead zone). It was highlighted that the use of two sensorized fingers enables to detect the contact side and to estimate the contact force. The contact force (F_y) control between the micropart and the rail enables to correct the trajectory when the contact appears. An incremental control is proposed and it produces a residual contact force due to the dead zone which does not destabilize the grasp. Validation setups and experimental results have been presented to validate the principle of the guiding task by two sensorized fingers. These works can be applied to automated micro-assembly tasks by controlling forces in the range of 10 μN to 3 mN. Future works will focus on complete hybrid force/position control and dynamic force/position control of guiding tasks.

Acknowledgment

This work has partially been supported by the Franche-Comté region. The authors would like to thank Micky Rakotondrabe and Eric Descourvières for discussions, and David Guibert for his technical support.

References

[1] D. Tolfree and M. J. Jackson, *Commercializing Micro-Nanotechnology Products*. CRC Press, 2006.

[2] M. R. Descour, A. H. O. Kärkkäinen, J. D. Rogers, and C. Liang, "Toward the development of miniaturized imaging systems for detection of pre-cancer," *IEEE Journal of Quatum Electronics*, vol. 38, pp. 122–130, 2002.

[3] S. Rathmann, A. Raatz, and J. Hesselbach, *Concepts for Hybrid Micro Assembly Using Hot Melt Joining*. Springer Boston, 2008, pp. 161 – 169.

[4] N. Dechev, W. Cleghorn, and J. Mills, "Microassembly of 3-d microstructures using a compliant, passive microgripper," *Journal of Microelectromechanical Systems*, vol. 13, pp. 176 – 189, 2004.

[5] Z. Lu, P. C. Y. Chen, A. Ganapathy, G. Zhao, J. Nam, G. Yang, E. Burdet, C. Teo, Q. Meng, and W. Lin, "A force-feedback control system for micro-assembly," *Journal of Micromech. Microeng*, vol. 16, pp. 1861–1868, 2006.

[6] S. Fahlbusch and S. Fatikow, "Micro force sensing in a micro robotic system," in *IEEE International Conference on Robotics and Automation*, 2001, pp. 3435– 3440.

[7] M. Gauthier, S. R. P. Rougeot, and N. Chaillet, "Forces analysis for micromanipulations in dry and liquid media," *Journal of Micromechatronics*, vol. 3, pp. 389–413, 2006.

[8] K. Rabenorosoa, C. Clévy, P. Lutz, M. Gauthier, and P. Rougeot, "Measurement setup of pull-off force for planar contact at the microscale," *Micro Nano Letters*, vol. 4, pp. 148 –154, 2009.

[9] R. Volpe and P. Khosla, "A theoretical and experimental investigation of impact control for manipulators," *IEEE Trans. on Automatic Control*, vol. 12, pp. 351–365, 1993.

[10] Y. Zhou, B. J. Nelson, and B. Vikramaditya, "Fusing force and vision feedback for micromanipulation," in *IEEE International Conference on Robotics and Automation*, 1998, pp. 1220– 1225.

[11] Y. Shen, N. X, and W. J. Li, "Contact and force control in microassembly," in *IEEE International Symposium on Assembly and Task Planning*, 2003, pp. 60–65.

[12] F. Arai, D. Andou, Y. Nonoda, T. Fukuda, H. Iwata, and K. Itoigawa, "Integrated microendeffector for micromanipulation," *IEEE/ASME Trans. on Mechatronics*, vol. 3, pp. 17 – 23, 1998.

[13] M. C. Carrozza, A. Eisinberg, A. Menciassi, D. Campolo, S. Micera, and P. Dario, "Towards a force-controlled microgripper for assembling biomedical microdevice," *Journal of Micromech. Microeng*, vol. 10, pp. 271– 276, 2000.

[14] J. Wason, W. Gressick, J. T. Wen, J. Gorman, and N. Dagalakis, "Multi-probe micro-assembly," in *IEEE Conference on Automation Science and Engineering*, 2007, pp. 63–68.

[15] F. Beyeler, A. Neild, S. Oberti, D. J. Bell, Y. Sun, J. Dual, and B. J. Nelson, "Monolithically fabricated microgripper with integrated force sensor for manipulating microobjects and biological cells aligned in an ultrasonic field," *Journal of Microelectromechanical Systems*, vol. 16, pp. 7–16, 2007.

[16] W. H. Lee, B. H. Kang, Y. S. Oh, and H. Stephanou, "Micropeg manipulation with a compliant microgripper," in *IEEE International Conference on Robotics and Automation*, 2003, pp. 3213– 3218.

[17] Y. Li, "Hybrid control approach to the peg-in hole problem," *IEEE Robotics and Automation Magazine*, vol. 4, pp. 52– 60, 1997.

[18] G. Yang, J. A. Gaines, and B. J. Nelson, "A flexible experimental workcell for efficient and reliable wafer-level 3d microassembly," in *IEEE International Conference on Robotics and Automation*, 2001, pp. 133–138.

[19] K. Rabenorosoa, C. Clévy, P. Lutz, S. Bargiel, and C. Gorecki, "A micro-assembly station used for 3d reconfigurable hybrid moems assembly," in *IEEE International Symposium on Assembly and Manufacturing*, 2009.

[20] M. Raibert and J. Craig, "Hybrid position/force control of manipulators," *Transactions of ASME*, vol. 102, 1981.